Journal for
ImmunoTherapy of Cancer

Subtype and grade-dependent spatial heterogeneity of T-cell infiltration in pediatric glioma

M Hope Robinson ,[1] Juan Vasquez,[2] Akhilesh Kaushal,[3] Tobey J MacDonald,[4] José E Velázquez Vega,[1] Matthew Schniederjan,[1] Kavita Dhodapkar [4]

[1]Pediatrics, Emory University School of Medicine, Atlanta, Georgia, USA
[2]Pediatric Oncology, Yale University, New Haven, Connecticut, USA
[3]Hematology and Medical Oncology, Emory University School of Medicine, Atlanta, Georgia, USA
[4]Aflac Cancer and Blood Disorders Center, Children's Healthcare of Atlanta, Department of Pediatrics, Emory University, Atlanta, Georgia, USA

Correspondence to
Dr Kavita Dhodapkar;
kavita.dhodapkar@emory.edu

ABSTRACT

Brain tumors are the leading cause of cancer-related mortality in children and have distinct genomic and molecular features compared with adult glioma. However, the properties of immune cells in these tumors has been vastly understudied compared with their adult counterparts. We combined multiplex immunofluorescence immunohistochemistry coupled with machine learning and single-cell mass cytometry to evaluate T-cells infiltrating pediatric glial tumors. We show that low-grade tumors are characterized by greater T-cell density compared with high-grade glioma (HGG). However, even among low-grade tumors, T-cell infiltration can be highly variable and subtype-dependent, with greater T-cell density in pleomorphic xanthoastrocytoma and ganglioglioma. CD3+ T-cell infiltration correlates inversely with the expression of SOX2, an embryonal stem cell marker commonly expressed by glial tumors. T-cells within both HGG and low-grade glioma (LGG) exhibit phenotypic heterogeneity and tissue-resident memory T-cells consist of distinct subsets of CD103+ and TCF1+ cells that exhibit distinct spatial localization patterns. TCF1+ T-cells are located closer to the vessels while CD103+ resident T-cells reside within the tumor further away from the vasculature. Recurrent tumors are characterized by a decline in CD103+ tumor-infiltrating T-cells. BRAF[V600E] mutation is immunogenic in children with LGG and may serve as a target for immune therapy. These data provide several novel insights into the subtype-dependent and grade-dependent changes in immune architecture in pediatric gliomas and suggest that harnessing tumor-resident T-cells may be essential to improve immune control in glioma.

BACKGROUND

Brain tumors are the most common pediatric solid tumor and a leading cause of cancer-related mortality in children.[1] These tumors exhibit considerable heterogeneity in terms of their histopathology, grade, clinical presentation and outcome, with low-grade tumors representing the most common subtypes. Surgical resection (if feasible), radiation and chemotherapy represent common approaches to treat these tumors, but carry significant risk of recurrent disease and long-term morbidity. Therefore, newer approaches to treat these tumors are being explored.

Molecular alterations in BRAF, including mutations (BRAF[V600E]) as well as fusions (BRAF-KIAA1549), lead to MAPK pathway activation, an important driver of tumorigenicity in pediatric glioma.[2] Importance of BRAF signaling in these tumors is further supported by clinical responses to BRAF kinase inhibitors.[3] However, response to BRAF kinase inhibitors are rarely curative, seen in only a proportion of patients, require long-term therapy and are expected to lead to drug resistance based on experience with other tumors such as melanoma.[4]

The immune system has emerged as a powerful tool to treat human tumors. Immune therapies, and particularly those that reactivate pre-existing immunity via blockade of inhibitory immune checkpoints, have shown considerable promise in several tumor types. It is now increasingly appreciated that the nature of tumor-infiltrating immune cells impact responsiveness to such therapies and outcome. Several studies have evaluated the attributes of immune and other cells infiltrating adult glial tumors.[5] These studies reveal a tumor immune environment dominated by myeloid cell infiltration and a paucity of T cells. Studies of adult glioma also reveal a number of tumor-suppressive factors, including cytokines such as TGF-β and IL-10, myeloid-derived suppressor cells and regulatory T cells, as well as immune-suppressive metabolites such as IDO present within these tumors.[6] This has also led to several approaches to target the inhibitory cells and molecules. and harness the immune system to treat brain tumors in adults.[6 7] It is increasingly appreciated that glial tumors in children have distinct genetic and molecular features as well as characteristic biological behaviors when compared with their adult tumors.[3 8 9]
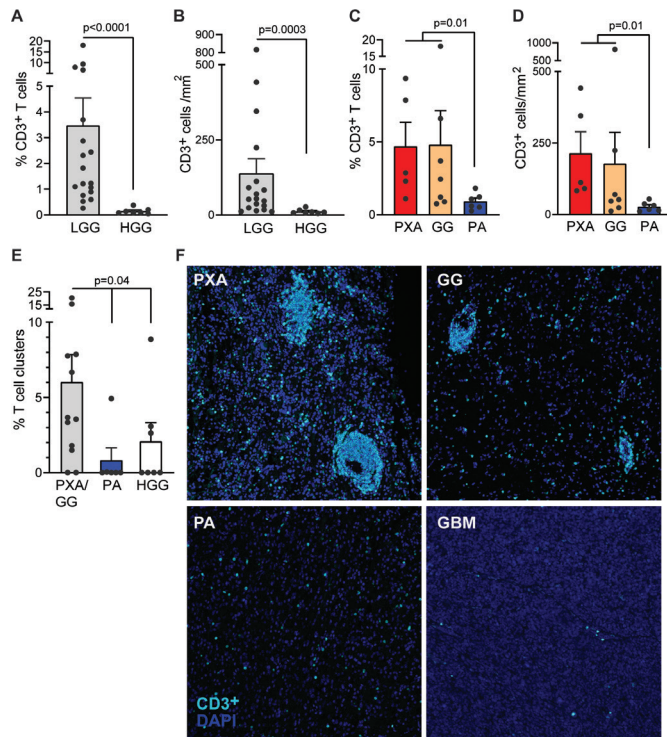
Figure 1 Subtype-dependent and grade-dependent changes in T-cell infiltration in pediatric gliomas. Tumors from patients with LGG (including PXA (n=5), GG (n=7) and PA (n=6)) and HGG (including anaplastic astrocytoma (n=2) and GBM (n=5)) were examined using multiplex immunohistochemistry. (A) CD3 T cells as a percentage of total cells in LGG (PXA, GG and PA) versus those in HGG (AA and GBM). (B) T-cell density in LGG and HGG tumor tissue. (C) Percentage of CD3+ T cells in different LGG subtypes (PXA, GG and PA). (D) CD3+ T-cell density in different LGG subtypes (PXA, GG and PA). (E) Percentage of T cells in clusters in PXA and GG, and PA and HGG. (F) Representative sections from patients with PXA, GG, PA and GBM showing distribution of T cells in tumor tissue. All graphs show mean, and SEM dots represent individual patient values. GBM, glioblastoma multiforme; AA, anaplastic astrocytoma; GG, ganglioglioma; HGG, high-grade glioma; LGG, low-grade glioma; PA, pilocytic astrocytoma; PXA, pleomorphic xanthoastrocytoma .

However, the nature of immune cells infiltrating pediatric brain tumors are vastly understudied compared with their adult counterparts.

Success of T-cell immune checkpoint blockade in the clinic has led to increased focus on the T-cell compartment within tumors. Recent advances in the biology of memory T cells in the setting of chronic infections as well as immunity in non-lymphoid tissues has led to an appreciation of distinct subsets of T cells in tumor immunity and response to checkpoint blockade.[10 11] In prior studies, we and others have shown that the expression of immune checkpoints such as PD-1 is enriched in the subset of T cells within tumors that express markers associated with tissue-resident memory (T_{RM}) cells.[12–14] The presence of T_{RM} cells within tumors has been linked to response and survival following immune therapies.[12] Another subset of 'stem-like' memory T cells has also been implicated in response to checkpoint blockade and detected within human tumors.[15 16] However, the spatial aspects, phenotype and overlap between these populations have not been directly compared.

In order to address these issues, we combined multiplex immunohistochemistry (IHC), machine learning and single-cell mass cytometry to better understand the phenotype and spatial localization of immune cells in pediatric brain tumors, with a focus on the T-cell compartment.

RESULTS AND DISCUSSION

In order to gain initial insights into the nature of T-cell infiltration within pediatric tumors of diverse types, we stained tissues from 26 pediatric tumors (18 low grade and 8 high grade, patient characteristics in online supplementary table 1). Low-grade tumors were characterized by greater CD3+ T-cell infiltration (figure 1A) as well as CD3+ T-cell density (figure 1B) compared with high-grade tumors. However, even within low-grade tumors, T-cell infiltration was found to be highly variable and subtype-dependent, with higher CD3+ T-cell infiltration and T-cell density in two specific subtypes, pleomorphic xanthoastrocytoma (PXA) and ganglioglioma (GG) (figure 1C and D). One aspect of T-cells within tissues is their tendency to cluster together, particularly at sites of antigenic stimulation. In order to quantify T-cell proximity, we analyzed the proportion of T-cells with greater than ten (>10) other T-cells close to them within a 30 micron radius. Both PXA and GG subtypes had a higher proportion of such clusters compared with pilocytic astrocytoma (PA) or high-grade glioma (HGG) (figure 1E–F). Together, these data demonstrate subtype-dependent heterogeneity of T-cell infiltration in pediatric gliomas and identify PXA and GG as subtypes associated with greater T-cell infiltration.

In order to better characterize the nature of infiltrating immune cells at greater depth, we used single-cell mass cytometry or CyTOF (see online supplementary table 2 for antibodies used in the panels) to analyze tumor-infiltrating immune cells from patients with gliomas using available fresh tissue. Analysis of tumors from a cohort of nine patients (online supplementary table 1B) demonstrated that the T-cells within glial tumors consisted predominantly of CD69+ and CD45RO+ cells (figure 2A), consistent with the phenotype commonly ascribed to T_{RM}. These T_{RM} cells could be split into three distinct subsets based on the expression of CD103 and TCF1 (figure 2B–2D). The subset of CD69+CD103+memory T-cells expressed the highest levels of inhibitory checkpoints such as PD-1 and TIGIT, and consisted predominantly of CD8+ T-cells expressing lytic markers such as granzyme B (figure 2B–2D). In contrast, the TCF1+ subset consisted of both CD4 (predominant) and CD8+ T-cells, and was characterized by higher expression of CD127 (figure 2B–D). These distinct subsets of T-cells could also be detected by multiplex immunofluorescence IHC, and tumors with
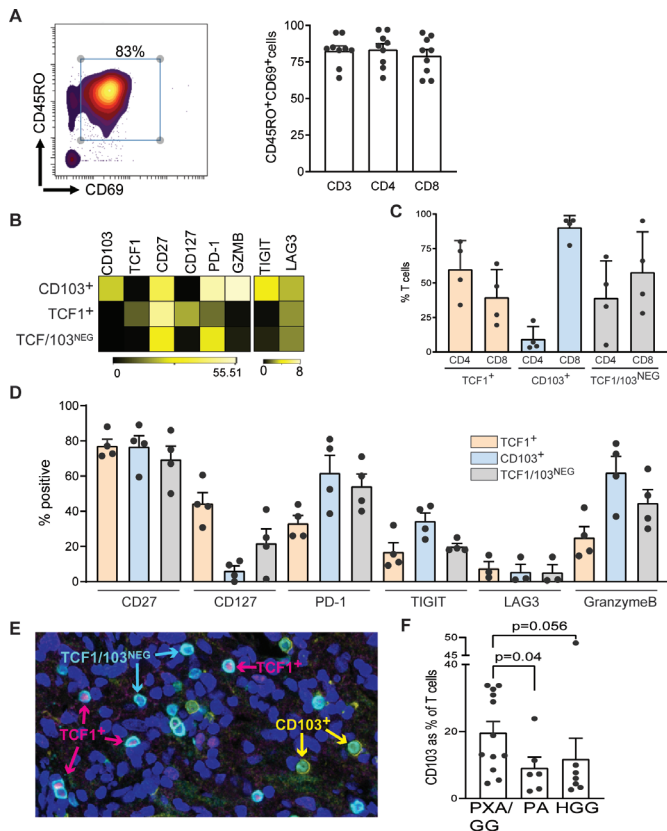
Figure 2 Phenotypic heterogeneity of glioma-infiltrating T cells. (A to D) Single-cell mass cytometry was performed on freshly isolated tumor tissue from pediatric glioma samples to characterize the tumor infiltrating T cells. (A) CD3-gated density plot showing expression of CD45RO and CD69 on tumor-infiltrating T cells. Bar graph shows CD69+, CD45RO+ and TRM cells as percent of total CD3, CD4 and CD8 T cells in all patients (n=9). (B) Heatmap showing expression of CD103, TCF1, CD27, CD127, PD-1, GZMB, TIGIT and LAG3 in CD103+, TCF1+ and TCF1/CD103^{neg} T cells (n=4). (C) Bar graph showing distribution of CD4 and CD8 T cells within CD103+, TCF1+ and TCF1/CD103^{neg} T cells (n=4). (D) Bar graph shows expression of CD27 and CD127, inhibitory immune checkpoints PD-1, TIGIT and LAG3, and GZMB in CD103+, TCF1+ and TCF1/CD103^{neg} T cells (n=4). (E and F) Panels show multiplex IHC was used to characterize the expression of TCF1 and CD103 on tumor-infiltrating T cells. (E) Major subtypes of T cells identified by multiplex IHC of paraffin-embedded tumor tissue included CD3+ and TCF1+ T cells, CD3+ and CD103+ T cells, and CD3+, CD103^{neg} and TCF1^{neg} T cells (n=26). (F) CD103+ and CD3+ T cells as percent of total CD3+ T cells in PXA/GG as well as in patients with PA and HGG as determined by multiplex IHC. All graphs show mean and SEM dots represent individual patient values. GG, ganglioglioma; GZMB, granzyme B; HGG, high-grade glioma; IHC, immunohistochemistry; PA, pilocytic astrocytoma; PXA, pleomorphic xanthoastrocytoma.

PXA/GG subtypes had the highest proportion of T-cells with CD103+ T$_{RM}$ phenotype (figure 2E–F).

Interestingly, in addition to phenotypic differences between the major T-cell subsets in glioma tissue, we also observed surprising differences in their spatial distribution. In general, T-cells were observed within both
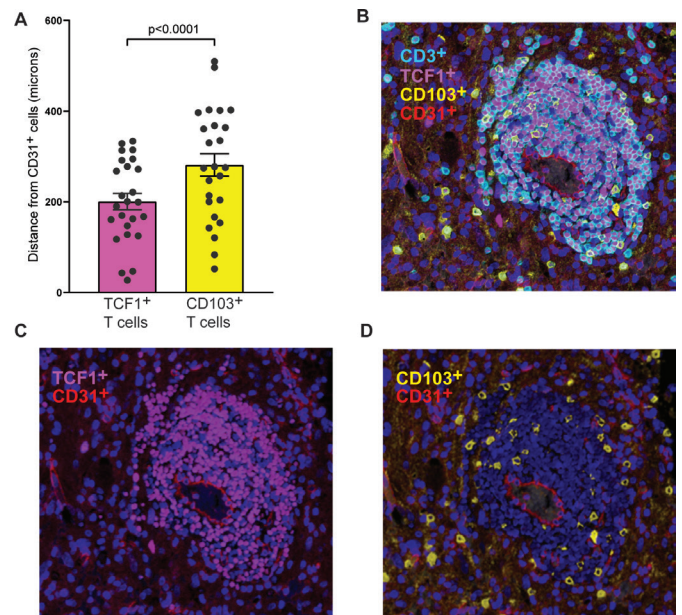

Figure 3 Spatial heterogeneity of T-cell subsets in glioma tissue. (A) Bar graph showing the distance of TCF1+ and CD103+ T-cells from CD31+ endothelial cells (in microns). Bar graph shows mean and SEM (n=25). (B to D). Representative images showing differential spatial distribution of TCF1+ and CD103+ T-cells in glioma tissue. The endothelium is labeled by CD31+ cells.

perivascular as well as intratumoral locations. However, there was a distinct difference in the spatial localization of the T-cell subsets, with TCF1+ cells enriched in the perivascular locations, while the CD103+ T-cells were also observed within the tumors and further away from the vessels (figure 3). In order to quantify this in an unbiased fashion, we used machine learning to assess distance of individual T-cells from CD31+ cells as a surrogate marker for endothelium. The mean distance between TCF1+ T-cells and CD31+ cells was significantly lower than that for CD103+ T-cells and CD31+cells (figure 3A; representative images in figure 3B–D).

In spite of a generally excellent prognosis, patients with low-grade tumors may experience recurrent disease, often at the site of initial tumor. In the case of three PA tumors, we had access to tissues at initial diagnosis as well as at recurrence (online supplementary table 1C). As noted earlier, PA tumors had a lower proportion of CD103+ T-cells at baseline. However, comparison of tissues at recurrence revealed a further decline in CD103+ tissue-resident T cells, as well as an increase in CD31+ cells, indicative of increased vascularity in recurrent tumors compared with that at initial diagnosis (figure 4A and B).

In prior studies with solid tumors, the degree of T-cell infiltration has been correlated with stem-like features of tumor cells, angiogenesis and particularly with a high tumor mutational burden.[17] The finding that PXA/GG subtypes have a high degree of T-cell infiltration is therefore surprising because these tumors have a very low mutational burden. SOX2 has emerged as an important tumor stem-cell marker in human glial tumors.[18–20] HGG were associated
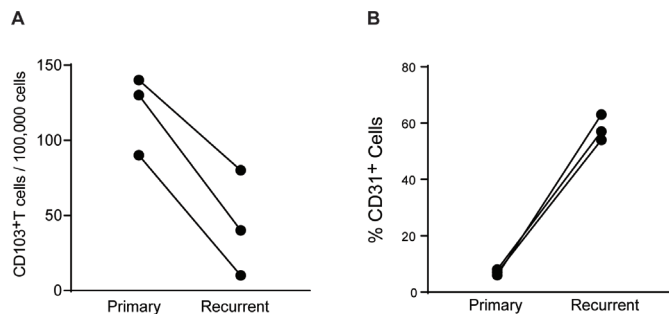
Figure 4 Recurrent pilocytic astrocytoma is characterized by increased vascularity and a decline in CD103+ T_{RM} cells. Comparison of CD103+ T-cells and CD31+ endothelial cells in paired tissues at initial diagnosis and at relapse in three patients with pilocytic astrocytoma. (A) Changes in CD103+ T-cells at recurrence. (B) Changes in CD31+ endothelial cells at recurrence.

with higher expression of SOX2 compared with low-grade glioma (LGG) (online supplementary figure 1A). Interestingly, the presence of T-cells within tumors was inversely correlated with the expression of SOX2 (online supplementary figure 1B). Although most pediatric LGG share activation of the BRAF-MAPK pathway as a common genomic alteration,[8] the mechanism underlying BRAF activation in PXA/GG is commonly the V600E mutation, while BRAF-KIAA1549 fusion is observed in PAs.[8] T-cells against driver mutations have been limited in some settings, presumably due to selection based on HLA genotype.[21] In order to test whether the BRAF[V600E] mutation could be immunogenic in pediatric tumors, we synthesized peptides encompassing this mutation and used these to detect and expand BRAF[V600E]-specific T-cells in culture. In a patient with BRAF[V600E]-mutant LGG and available fresh T-cells, we could demonstrate the presence of V600E-specific T-cell immunity (online supplementary figure 2A). In a different patient with a BRAF[V600E]-mutant anaplastic GG (classified as HGG, online supplementary table 1B), while we did not detect BRAF[V600E] mutation-specific T-cells in freshly isolated T-cells, we could demonstrate expansion of BRAF[V600E]-specific T-cells after stimulation with autologous dendritic cells pulsed with mutant peptide (online supplementary figure 2B).

These data provide several novel insights into the nature of T-cell infiltration within pediatric brain tumors, with potential biologic and clinical implications. First, our data show that there is marked subtype-dependent variation in the degree of T-cell infiltration even within low-grade glial tumors in children, with two subtypes, PXA and GG, associated with a particularly high degree of T-cell infiltration. The brain is typically viewed as an immune-privileged site and not routinely surveyed by lymphocytes. Indeed, brain tumors, particularly in adults, have been studied as classic examples of immunologically cold tumors. Our data, however, identify PXA and GG as distinct subtypes that break this paradigm. These subtypes, although rare, may therefore be excellent candidates for immune therapies and a better understanding of their biology may provide fundamental insights into improving immune therapy of glioma. One target of

T-cell responses may be the BRAF[V600E] mutation itself, as we could document immunogenicity of this mutation. Small molecule BRAF inhibitors can lead to tumor regression in such tumors, but resistance evolves without the loss of mutant protein suggesting that these tumors may remain susceptible to T-cell therapy.[22] Clinical response to such therapy has been reported in a melanoma patient,[23] and our studies set the stage for consideration of neoantigen-directed T-cell therapy in BRAF[V600E]-mutant pediatric glioma.

The presence of T-cell infiltration was inversely correlated with the expression of SOX2, an embryonal stem cell marker commonly expressed on glial tumor cells and associated with stemness and clonogenic potential in glial tumors.[18 19] This is particularly true when patients with HGG are considered, as they often express high levels of SOX2 and appear to be poorly infiltrated with T-cells. Whether the expression of these stemness markers contributes to exclusion of immune infiltration in glioma deserves further study, as targeting this gene may then enhance glioma immune therapies.

Limitations of our study include small sample size and the lack of clinical follow-up data to understand the importance of the spatial location of the TCF1+ and CD103+ tumor-resident T-cells. In addition, while we could detect BRAF[V600E] mutation-specific T-cells in pediatric glioma, we were not able to test lysis of autologous tumors by these T-cells. Our data also do not address the potential immunogenicity of other (non-V600E) alterations in the BRAF pathway in these patients.

Our data provide novel insights into spatial aspects of heterogeneity of tumor-infiltrating lymphocytes in pediatric tumors, with identification of two major subtypes: TCF1+ T-cells mostly in the perivascular location and CD103+ T-cells within the tumor. The subset of CD103+ T-cells within tumors is of particular interest, as this subset has been implicated in pathogen-specific tissue immunity and long-term protection in mouse models of viral central nervous system infection.[24 25] In these models, such T-cells persist long term within tissue, without replenishment from circulation. Our finding that recurrent LGG are characterized by a loss of CD103+ T-cells suggests that strategies to enhance these T-cells in situ, such as intracranial dendritic cell immunization explored in preclinical studies, may be worthy of exploration.[25] Recurrent tumors were also characterized by increased angiogenesis, which is consistent with prior studies correlating angiogenic factors such as VEGF (vascular endothelial growth factor) and loss of T_{RM},[14 26 27] and support consideration of targeting these factors in combination with immune therapies to treat recurrent tumors.

METHODS
Patients and tissues
Formaldehyde-fixed paraffin-embedded tumor blocks were obtained from de-identified pediatric glioma. In three patients with PA, sections were also obtained from paired tumor blocks from initial diagnosis as well as recurrence. Institutional IRB approved (Emory and Yale University) informed consent/parental permission

and when possible, child assent was obtained prior to receiving fresh tissue or peripheral blood samples. All tissue diagnoses were confirmed by study pathologists and were based on 2016 WHO criteria with cIMPACT-NOW recommendations when appropriate.

Multiplex immunofluorescence IHC
Sections were cut at 5 µM thickness and mounted on positively charged slides for staining. H&E slides were evaluated by a neuropathologist (MS) to confirm areas of tumor. Opal (Akoya Biosciences) multiplex staining using a Ventana DISCOVERY ULTRA system (Roche) autostainer was performed by staining tissue sections with antibodies to detect SOX2, CD3, CD103, TCF1, CD31 and DAPI simultaneously (antibody panel is shown in online supplementary table 3). Deparaffinization was accomplished with heat and EZ-Prep solution, followed by application of Cell Conditioning 1 (CC1, Roche). Blocking of endogenous peroxidase activity was performed with DISCOVERY Inhibitor (Roche). Antibody staining was achieved in an iterative manner with antibodies applied in the order indicated in online supplementary table 2. After primary antibody incubation, species appropriate horseradish peroxidase (HRP)-conjugated secondary antibody (DISCOVERY OmniMap anti-mouse HRP (760–4310) or anti-rabbit HRP (760–4311), Roche) was applied followed by application of the tyramide signal amplification Opal dye. Denaturing of the primary and secondary antibodies was accomplished by heating at 93°C with Cell Conditioning 2 (CC2, Roche). Counter staining of nuclei was achieved using Spectral DAPI (Akoya). Slides were coverslipped with VECTASHIELD Antifade mounting medium (Vector Laboratories). Stained slides were stored at 4°C.

Analysis of IHC data
Images of stained slides were acquired with the Vectra Polaris (Akoya Biosciences) whole-slide scanner using a standardized scanning protocol. Software fluorophore signal unmixing and removal of autofluorescence followed by digital image analysis was accomplished with inForm software (Akoya Biosciences). Representative fields from each sample were used for training of inForm machine learning software to segment different areas of tissue and individual cells. Training of cell phenotyping was accomplished using a layered approach, training each marker separately to obtain optimal range of expression for each marker while excluding overlapping cells. The algorithms created during this training were then used to analyze all tumor areas on each slide. The resulting data, including tissue and cell segmentation, cell phenotyping and cell positions allowing for distance calculations were then analyzed using Phenoptr and Phenoptr Reports (add-ins for R Studio from Akoya Biosciences).

Mass cytometry
Fresh tumor tissue was dissociated to obtain single-cell suspension and stained using 36 metal tagged antibodies as previously described using the manufacturers protocols.[14] Cell viability staining was detected by Cell-ID Cisplatin and MaxPar Intercalator-Ir was used to detect intact cells before acquiring on the Helios instrument (DVS Sciences; Fluidigm). To facilitate quantitative comparisons between data acquired on different days, single-cell data was normalized using beads. All data were analyzed using Cytobank. The antibodies and their clones and vendors are shown in online supplementary table 2.

Peptide libraries
15-mer BRAF wild-type and mutated BRAF^{V600E} peptides were synthesized by the Proteomics Resource Center at The Rockefeller University, as previously described.[28] The mutated residue was placed at position +7 of the 15 amino acid sequence. All peptides were reconstituted in DMSO. A pool of peptides derived from cytomegalovirus, Epstein-Barr virus and influenza virus (CEF; AnaSpec Inc) were used as a positive control.

Detection of antigen-specific T cells
The presence of BRAF-reactive T cells was detected based on antigen-dependent cytokine production, as previously described.[13] Briefly, peripheral blood mononuclear cells were cultured either with media alone (control) or together with CEF peptides (5 µg/mL per peptide) or BRAF wild-type and BRAF^{V600E} peptides (10 µg/mL per peptide) in 5% PHS, in 96-well round bottom plates (2.5×10^5 cells/well). PHA was used as an additional positive control. After 48 hours, culture supernatants were harvested and examined for the presence of chemokine (C-X-C motif) ligand 10 (CXCL10) using a Luminex assay, as per manufacturer's instructions (Millipore, Massachusetts, USA). Presence of CXCL10 was detected with Luminex 100 instrument and analyzed using the xPONENT software (Luminex Corporation). Values ≥2-fold over the negative control were deemed positive, based on the analysis of inter-assays and intra-assays variation, as previously described.[13 29] In this assay, the antigen-induced secretion of CXCL10 (or IP-10, interferon-induced protein 10) serves as a downstream marker of T-cell derived IFN-γ and is abrogated by depletion of CD3+ T-cells and IFN-γ neutralization, as previously described.[29]

Generation of dendritic cells and antigen-specific T-cell expansion
Monocyte-derived dendritic cells (Mo-DCs) were generated using IL-4 and GM-CSF as previously described.[30] Day 6 immature Mo-DCs were loaded with BRAF wild-type peptides or BRAF^{V600E} peptides for 4 hours at 37°C, matured overnight with LPS (20 ng/mL) and used to stimulate autologous T-cells at a DC:T-cell ratio of 1:20 in the presence of IL-2 (10 IU/mL at days 4 and 7; Chiron) as well as IL-7 and IL-15 (both at 5 ng/mL at days 7 and 14, R&D). After 14 days in culture, the cells were re-stimulated using the peptides used for initial T-cell stimulation in the presence of soluble anti-CD28 and anti-CD49D

(1 µg/mL, BioLegend) and GolgiStop (BD Biosciences) for 5 hours at 37°C. Intracellular cytokine flow cytometry was used to detect intracellular IFN-γ.

Statistical analysis

Statistical analysis of IHC and mass cytometry data was performed using 2D graphing and statistics software GraphPad Prism. Non-parametric Mann-Whitney (for comparing two groups) was used for paired samples. Spearmans rank correlation between T-cell infiltration and SOX2 expression was calculated using R V.3.6.1 (online supplementary figure 1B).

ORCID iDs
M Hope Robinson http://orcid.org/0000-0002-4255-1308
Kavita Dhodapkar http://orcid.org/0000-0003-0587-4172

REFERENCES

1. Udaka YT, Packer RJ. Pediatric brain tumors. *Neurol Clin* 2018;36:533–56.
2. Packer RJ, Pfister S, Bouffet E, *et al*. Pediatric low-grade gliomas: implications of the biologic era. *Neuro Oncol* 2017;19:750–61.
3. Lassaletta A, Zapotocky M, Mistry M, *et al*. Therapeutic and prognostic implications of BRAF V600E in pediatric low-grade gliomas. *J Clin Oncol* 2017;35:2934–41.
4. Karoulia Z, Gavathiotis E, Poulikakos PI. New perspectives for targeting Raf kinase in human cancer. *Nat Rev Cancer* 2017;17:676–91.
5. Quail DF, Joyce JA. The microenvironmental landscape of brain tumors. *Cancer Cell* 2017;31:326–41.
6. Fecci PE, Sampson JH. The current state of immunotherapy for gliomas: an eye toward the future. *J Neurosurg* 2019;131:657–66.
7. Kelly WJ, Giles AJ, Gilbert M. T lymphocyte-targeted immune checkpoint modulation in glioma. *J Immunother Cancer* 2020;8:e000379.
8. Ryall S, Tabori U, Hawkins C. Pediatric low-grade glioma in the era of molecular diagnostics. *Acta Neuropathol Commun* 2020;8:30.
9. Jones DTW, Kieran MW, Bouffet E, *et al*. Pediatric low-grade gliomas: next biologically driven steps. *Neuro Oncol* 2018;20:160–73.
10. Amsen D, van Gisbergen KPJM, Hombrink P, *et al*. Tissue-resident memory T cells at the center of immunity to solid tumors. *Nat Immunol* 2018;19:538–46.
11. Hashimoto M, Kamphorst AO, Im SJ, *et al*. Cd8 T cell exhaustion in chronic infection and cancer: opportunities for interventions. *Annu Rev Med* 2018;69:301–18.
12. Dhodapkar KM. Role of tissue-resident memory in intra-tumor heterogeneity and response to immune checkpoint blockade. *Front Immunol* 2018;9:1655.
13. Vasquez JC, Huttner A, Zhang L, *et al*. SOX2 immunity and tissue resident memory in children and young adults with glioma. *J Neurooncol* 2017;134:41–53.
14. Boddupalli CS, Bar N, Kadaveru K, *et al*. Interlesional diversity of T cell receptors in melanoma with immune checkpoints enriched in tissue-resident memory T cells. *JCI Insight* 2016;1:e88955.
15. Bailur JK, McCachren SS, Doxie DB, *et al*. Early alterations in stem-like/resident T cells, innate and myeloid cells in the bone marrow in preneoplastic gammopathy. *JCI Insight* 2019;5. doi:10.1172/jci.insight.127807. [Epub ahead of print: 23 Apr 2019].
16. Sade-Feldman M, Yizhak K, Bjorgaard SL, *et al*. Defining T cell states associated with response to checkpoint immunotherapy in melanoma. *Cell* 2018;175:e1020:998–1013.
17. Zou W, Wolchok JD, Chen L. Pd-L1 (B7-H1) and PD-1 pathway blockade for cancer therapy: mechanisms, response biomarkers, and combinations. *Sci Transl Med* 2016;8:328rv324.
18. Favaro R, Appolloni I, Pellegatta S, *et al*. Sox2 is required to maintain cancer stem cells in a mouse model of high-grade oligodendroglioma. *Cancer Res* 2014;74:1833–44.
19. Hemmati HD, Nakano I, Lazareff JA, *et al*. Cancerous stem cells can arise from pediatric brain tumors. *Proc Natl Acad Sci U S A* 2003;100:15178–83.
20. Tam WL, Ng HH. Sox2: masterminding the root of cancer. *Cancer Cell* 2014;26:3–5.
21. Marty R, de Prisco N, Carter H, *et al*. MHC-I genotype drives early immune selection of oncogenic mutations. *Mol Cell Oncol* 2018;5:e1409863.
22. Shi H, Hugo W, Kong X, *et al*. Acquired resistance and clonal evolution in melanoma during BRAF inhibitor therapy. *Cancer Discov* 2014;4:80–93.
23. Veatch JR, Lee SM, Fitzgibbon M, *et al*. Tumor-Infiltrating BRAFV600E-specific CD4+ T cells correlated with complete clinical response in melanoma. *J Clin Invest* 2018;128:1563–8.
24. Wakim LM, Woodward-Davis A, Liu R, *et al*. The molecular signature of tissue resident memory CD8 T cells isolated from the brain. *J Immunol* 2012;189:3462–71.
25. Wakim LM, Woodward-Davis A, Bevan MJ. Memory T cells persisting within the brain after local infection show functional adaptations to their tissue of residence. *Proc Natl Acad Sci U S A* 2010;107:17872–9.
26. Das R, Verma R, Sznol M, *et al*. Combination therapy with anti-CTLA-4 and anti-PD-1 leads to distinct immunologic changes in vivo. *J Immunol* 2015;194:950–9.
27. Wallin JJ, Bendell JC, Funke R, *et al*. Atezolizumab in combination with bevacizumab enhances antigen-specific T-cell migration in metastatic renal cell carcinoma. *Nat Commun* 2016;7:12624.
28. Dhodapkar KM, Feldman D, Matthews P, *et al*. Natural immunity to pluripotency antigen Oct4 in humans. *Proc Natl Acad Sci U S A* 2010;107:8718–23.
29. Spisek R, Kukreja A, Chen L-C, *et al*. Frequent and specific immunity to the embryonal stem cell-associated antigen Sox2 in patients with monoclonal gammopathy. *J Exp Med* 2007;204:831–40.
30. Banerjee DK, Dhodapkar MV, Matayeva E, *et al*. Expansion of FOXP3high regulatory T cells by human dendritic cells (DCs) in vitro and after injection of cytokine-matured DCs in myeloma patients. *Blood* 2006;108:2655–61.